Conf-9009311

CONF-9009311--1

DE91 005012

ornl

OAK RIDGE NATIONAL LABORATORY

PHYSICS DIVISION PREPRINT

November 1990

Reactions Between Medium-Mass Nuclei at Subbarrier Energies

H. J. Kim
Oak Ridge National Laboratory,* Oak Ridge, Tennessee 37831-6372, U.S.A.

— *Invited Paper* —
Workshop on Low- and Medium-Energy Heavy-Ion Reactions
Kyoto, Japan, September 27–29, 1990

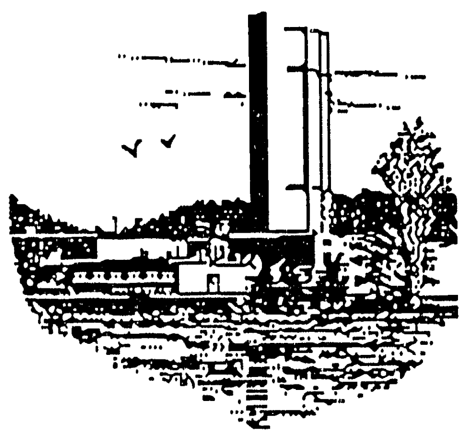

Conf-9009311

Reactions Between Medium-Mass Nuclei at Subbarrier Energies

H. J. Kim
Oak Ridge National Laboratory, Oak Ridge, Tennessee 37831-6372, U.S.A.*

A number of diverse theories can account, to a similar extent, for experimentally observed large enhancements in subbarrier fusion cross sections. For example, coupled-channels,[1] neck-formation,[2] distributed-barrier,[3] and direct absorption[4,5] theories have been used with comparable degrees of success to analyze the enhancement in $^{58}Ni+^{58}Ni$ fusion cross sections at subbarrier energies. This example illustrates that, although necessary, fusion cross sections alone are not sufficient to assess what really is the underlying enhancement mechanism.

Although their details vary, these theories share a reliance on interactions between the incident and one or more outgoing reaction channels to produce the enhancement. Being microscopic, the coupled-channels approach requires interactions with specific individual exit channels, such as inelastic and nucleon transfer. On the other hand, being macroscopic in nature, the neck-formation and distributed-barrier theories treat the interactions in a more global way. Thus, in addition to fusion, detailed studies of exit channels in general at subbarrier energies are very much needed in order to develop a good theoretical understanding of how the enhancement really comes about. However, only limited experimental data of this kind exist.

We present results from our study of transfer reactions between ^{50}Ti and ^{93}Nb that pertain to the subbarrier neck. Since the experimental arrangement used is the same as that of our previous study,[6] only a brief description is given. Target and target-like ejectiles emitted forward from the bombardment of thin ($\sim 30\ \mu g/cm^2$) ^{50}Ti targets by ^{93}Nb beams were first magnetically analyzed and then detected by a hybrid position-sensitive gas detector system, which was placed at the nominal focal plane of the magnet; ejectiles emitted at $10° \leq \theta \leq 20°$ angular range were investigated at bombarding energies of 283.1, 291.2, 273.2, 302.0, and 306.9 MeV. The c.m. angular range and energies are $140° \leq \theta \leq 160°$ (for elastics) and 99.0, 101.8, 103.9, 105.6, and 107.3 MeV. For reference, the potential barrier (Coulomb + centrifugal barriers) ranges from 108.0 MeV (at $E = 99.0$ MeV and $\theta = 160°$) to 111.2 MeV (at $E = 107.3$ MeV and $\theta = 140°$).

Only the products from the (^{50}Ti,^{49}Ti), (^{50}Ti,^{51}Ti), and(^{50}Ti,^{51}V) single-nucleon-transfer reactions were observed in the reaction-product spectra at $E_{c.m.} = 103.9$ MeV. Having a single peak, which is centered around the optimum transfer Q-value, the energy spectra for these single-nucleon-transfer reactions are normal at low energies. A drastic change occurs in the reaction product spectra at higher energies. This is illustrated in Fig. 1, where a reaction product spectrum at a slightly higher energy is shown. In addition to the abovenoted single-nucleon-transfer products, seven new products are seen in Fig. 1. Note that these new products result from channels requiring transfer of two or more nucleons, hereafter termed multinucleon transfer. Typical energy (or Q-value) spectra of the exit channels are shown in Figs. 2–4. The vertical line shown in each spectrum gives the position of the g.s.–g.s. transition (Q_{gg}). Noteworthy features of these spectra are: (1) single skewed peak with low-energy shoulder but centered or nearly centered around Q_{gg} dominates the incident and the three single-nucleon-transfer channel spectra; (2) a broad bump, located away from Q_{gg} by as much as ~ 10 MeV, characterizes all multinucleon-transfer channels; and (3) the difference between the average and g.s. g.s. Q-value generally increases with number of nucleons transferred.

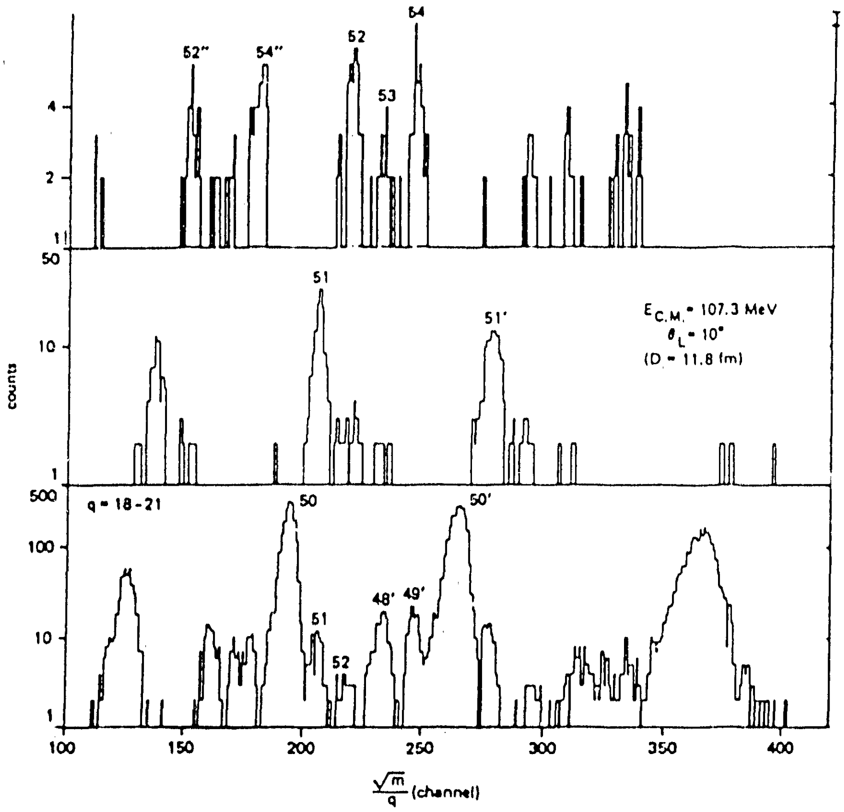

Fig. 1. Reaction product spectra. Numbers accompanying peaks identify Cr (top panel), V (center panel), and Ti (bottom panel) isotopes for most probable charge state q. Primed numbers are for adjacent q's.

For the present consideration, reaction probabilities and apsidal distances (internuclear distances at the classical turning point) are more appropriate than differential cross sections, energies, and angles. Accordingly, measured differential cross sections are converted to corresponding transfer probabilities. (A detailed discussion of this transformation can be found in Ref. 6.) Transfer probability P vs apsidal distance D plots for representative reactions are shown in Figs. 5 and 6. The straight lines that accompany the (^{50}Ti,^{49}Ti) and (^{50}Ti,^{51}V) single-nucleon-transfer results give the theoretical slopes (semi-log plots) as given by the low-energy transfer theory, namely the tunnelling theory (see Ref. 6, for example). Overall, experimental results do increase exponentially with decreasing D in a manner characteristic of the tunnelling process. Transfer probabilites for multinucleon-transfer channels are too small, and products from them were not observed for D larger than about 12.8 fm. This is illustrated by the (^{50}Ti,^{54}Cr) case in Fig. 6. However, the probability for all the multinucleon-transfer channels shown in Fig. 2 suddenly becomes large and products from these channels become observable beginning at about $D = 12.7$ fm, as illustrated in Fig. 6 for the (^{50}Ti,^{54}Cr) case. The magnitude of P for these channels are all similar for $D < 12.5$ fm.

The sudden appearance of a multitude of reaction products with comparable intensities is contrary to the tunnelling mechanism, i.e., based on observed $1p$- and $1n$-transfer intensities, the probability for transferring three or more nucleons is less 0.03% in the entire D range according to the tunnelling theory. One might argue that, if, for example, populated by cluster tunnelling (rather than by successive tunnelling), the probability for a particular channel can be as large as the observed value, since such an alternative transfer process is not related to single-nucleon-transfer processes. Even so, it is highly unlikely that all seven observed multinucleon-transfer channels happen to be populated by such mechanism. Nor is it likely that the magnitude of the resultant probabilities for seven different channels would be similar, even if the alternative mechanism did prevail. Furthermore, the average Q-values are much too negative relative to Q_{gg} for the multinucleon-transfer-products to result from the conventional mechanism.

The binary nature and the variety of exit channels populated and the damping in the kinetic energies are very reminiscent of characteristics one associates with the more familiar deep-inelastic reactions (see Wilczynski,[7] for example). In a typical deep-inelastic reaction, the formation of a quasi-molecule-like configuration follows the initial hard contact between the incident nuclei; and it is the subsequent decay of this configuration, which favors channels where some nucleon, energy and angular momentum were transferred, that populates binary exit channels. The kinetic energy is damped by the friction that accompanies the nucleon transfer while in the quasi-molecular configuration.

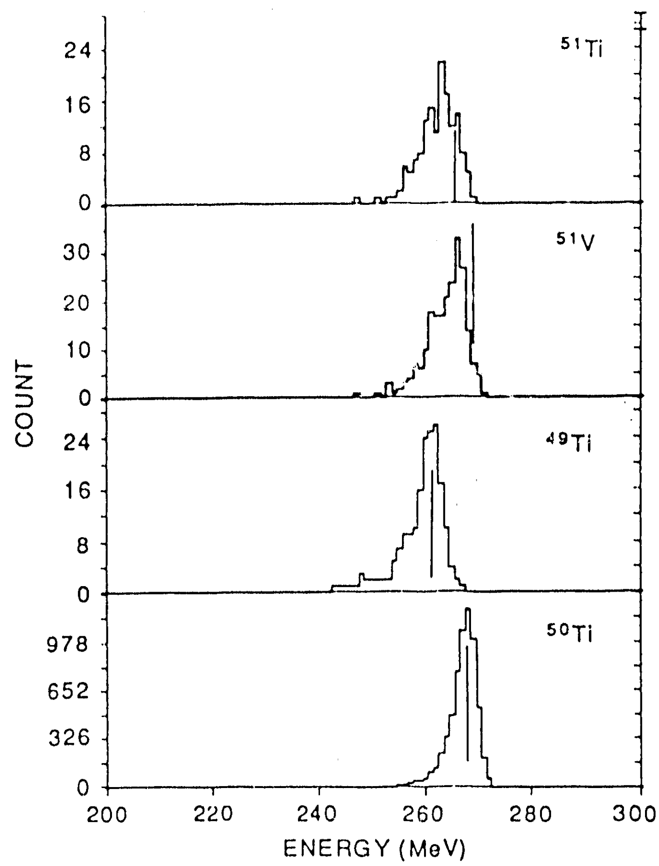

Fig. 2. Energy spectra for the incident and single-nucleon-transfer channels at $E_{c.m.}$ = 107.3 MeV and $\theta_L = 14°$. The heavy vertical lines show the positions of Q_{gg}.

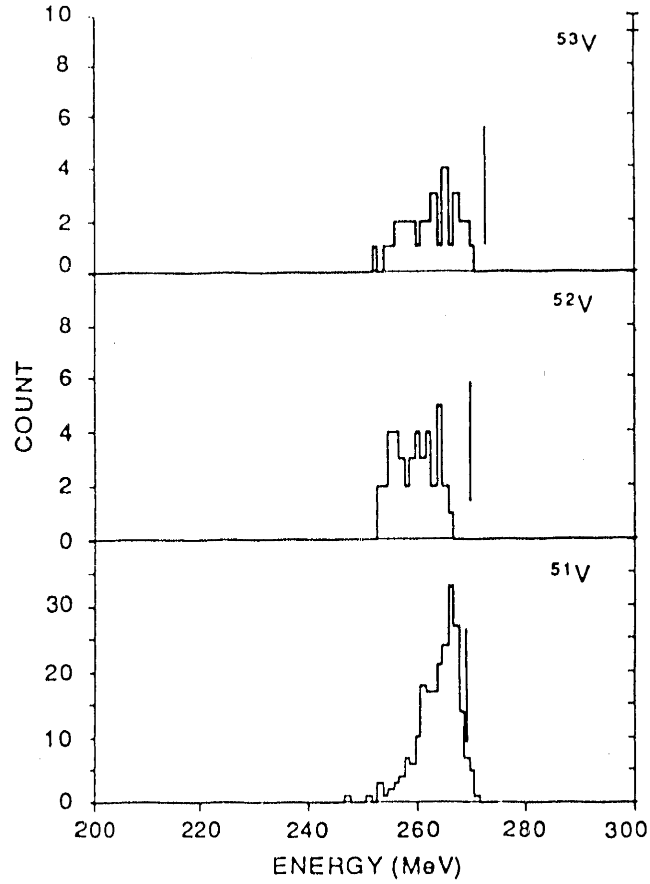

Fig. 3. Energy spectra of vanadium isotopes at $E_{c.m.}$ = 107.3 MeV and $\theta_L = 14°$.

Based on these close parallels between the present and the deep-inelastic reactions just noted, it is very tempting to associate the onset of the multinucleon-transfer reactions with the beginning, or early phase, of deep-inelastic reactions. There are, however, outstanding differences in circumstances of these reactions which counter or weaken this association. Foremost among these circumstances are the energy regime and the angular range. Deep-inelastic reactions typically occur at above-barrier energies, but the present reactions were observed at subbarrier energies; products from deep-inelastic reactions are confined to a narrow angular range near the grazing angle, but the present observations were restricted to large back angles. The difference in energy regimes implies a hard contact and a relatively small internuclear separation for deep-inelastic reactions vs a softer touch and larger separation for the subbarrier reactions; the difference in angular range pertains to a peripheral vs a more central collision.

A simple mechanism that gives a qualitative account of this as well as the fusion[8] experiment can be found in low-energy neck formation theories.[2,5] In these theories, a neck forms during a head-on collision between heavy ions at subbarrier energies, say, through liquid-drop effects, as the collision partners approach the turning point where they are separated by a certain critical distance. But the neck configuration eventually either coalesces or reseparates since it is not stable. Coalescence enhances fusion; reseparation enhances binary reactions. As for the case of deep-inelastic reactions, kinetic energies are damped by the friction encountered during the transfer process while in the neck-formed configuration.

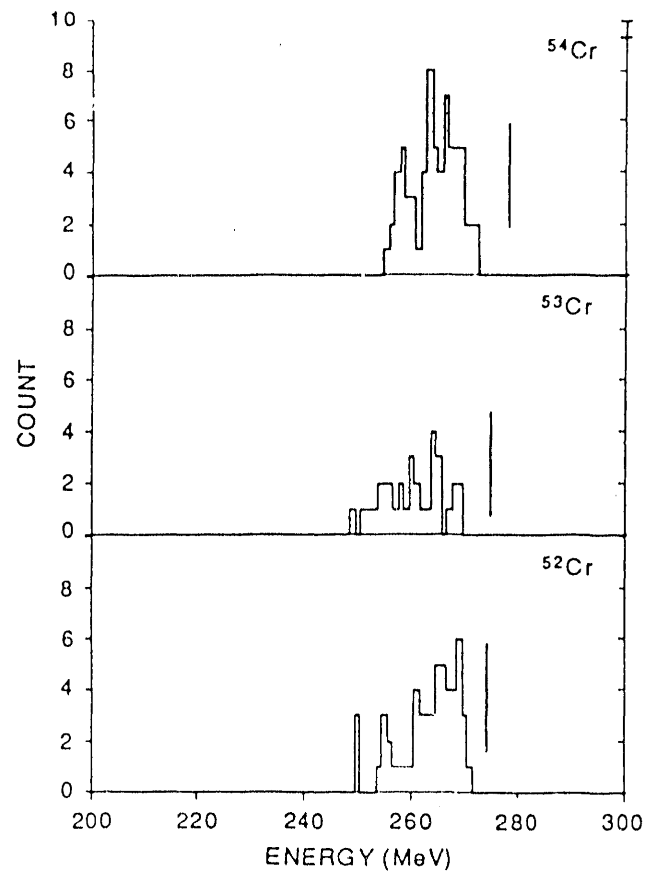

Fig. 4. Energy spectra of chromium isotopes at $E_{c.m.} = 107.3$ MeV and $\theta_L = 14°$.

A vital link connecting the above-described neck formation to quasi-elastic reactions was first suggested in Ref. 8. In Refs. 8 and 3, Stelson analyzed fusion cross-section data for projectiles ranging from ^{16}O to ^{64}Ni with the distributed-barrier model, where the fusion barrier is a distributed quantity with a well-defined threshold and mean, and found that the threshold energy required is closely correlated to the separation energy of the least-bound neutron of the projectile or target. From this finding, he suggested that neutron-transfer reactions precipitate the neck formation as follows. The mechanism for transferring the least-bound neutron switches from tunnelling to free flow beginning at the internuclear distance where the tunnelling probability first becomes 100% and thus saturates. The overlap of (neutron–nucleus) potentials becomes sufficient at this distance, and the tunnelling barrier vanishes for the neutron, permitting its free flow.

The fusion threshold determined from measured cross sections for the present system is 102.4 MeV, and the corresponding distance where the neutron free flow begins is 12.6 fm. As can be seen in Fig. 5, the onset of multinucleon-transfer reactions occurs near this distance also. The proximity of these distances is consistent with the neck formation being the underlying cause of enhancing, or boosting, multinucleon-transfer and fusion reactions and supports the suggestion that the neutron-transfer process is the catalytic reaction. In this connection, we note, in passing, that experimental results (fusion cross sections and the sum of transfer probabilities) indicate the neck configuration is as likely to reseparate as coalesce near the onset, or threshold.

Although a complete understanding of reactions reported here may be as yet unrealized, certain findings uncovered in this study can be exploited advantageously. As an example, consider the shape of ^{54}Cr and ^{89}Y nuclei at the moment of reseparation at a subbarrier energy. The average kinetic energy of this exit channel is less than that of the incident channel, although the Coulomb repulsion is stronger. In order for this to happen, the internuclear distance at the moment of separation must have been larger than the apsidal distance where the neck formed. This increase in distance necessarily implies that one or both of the exiting nuclei are very much elongated along the reseparation direction (prolate elongation). We have demonstrated that the ^{54}Cr+^{89}Y and other channels can be isolated cleanly. These channels are thus quite amenable to fragment gamma-ray coincidence studies that provide information pertaining to nuclear shape, energy division (between fragments), and fast vs slow elongation.

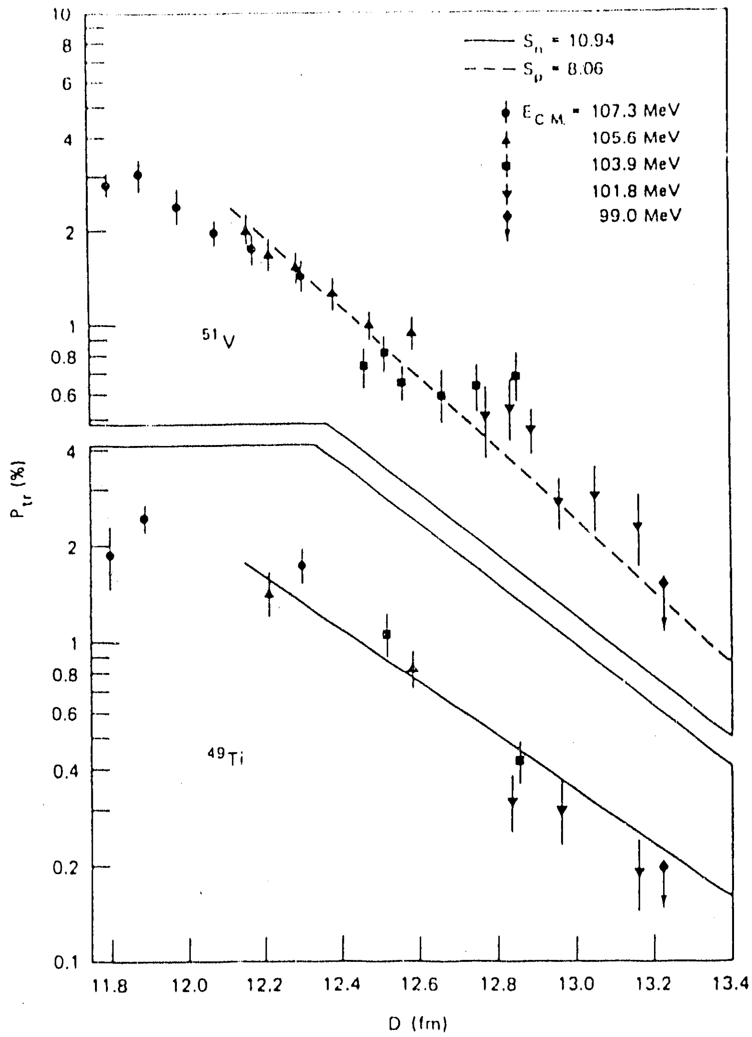

Fig. 5. Transfer probability vs apsidal distance for the $^{50}Ti \rightarrow {}^{49}Ti$ and $\rightarrow {}^{51}V$ reactions. Errors shown are statistical errors only. Upper limits only are shown for the lowest energy (99.0 MeV).

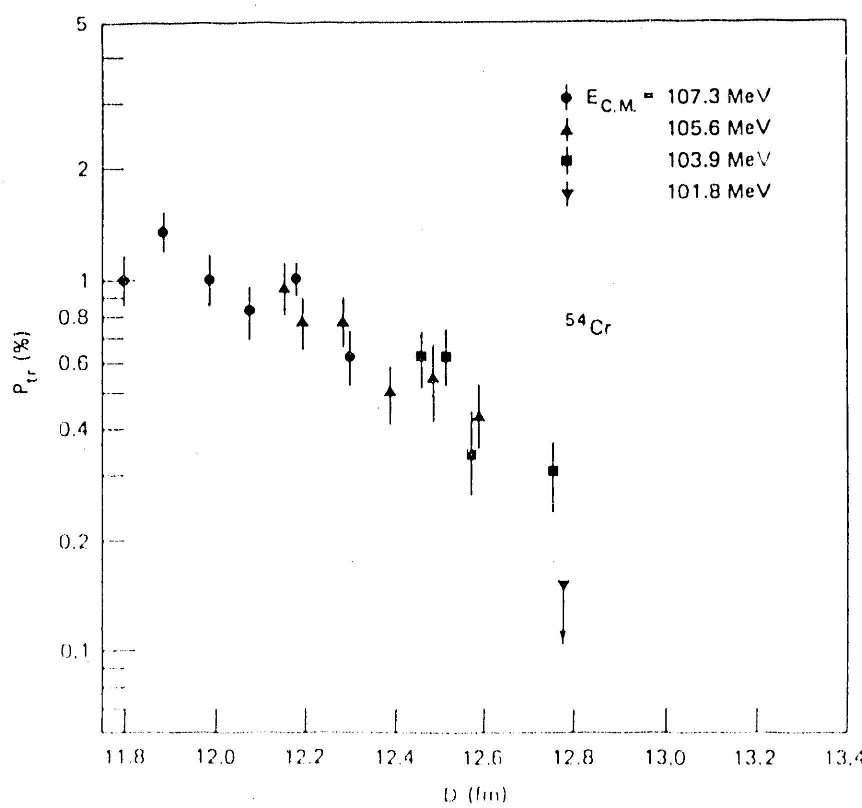

Fig. 6. Transfer probabilities for the $^{50}Ti \rightarrow {}^{54}Cr$ reaction. Errors shown are statistical errors only. Upper limit only is shown for the lowest energy (101.8 MeV).

References

* Operated by Martin Marietta Energy Systems, Inc., under contract DE-AC05-84OR21400 with the U.S. Department of Energy.
1. S. Landowne and S. C. Pieper, Phys. Rev. C **29**, 1352 (1984).
2. C. E. Aguiar *et al.*., Nucl. Phys. **A472**, 571 (1987); A. Iwamoto and K. Harada, Z. Phys. **A326**, 201, (1987); V. S. Ramamurthy *et al.*, Phys. Rev. C **41**, 2702 (1990).
3. P. H. Stelson, Phys. Lett. B **205**, 190 (1988).
4. T. Udagawa, B. T. Kim, and T. Tamura, Phys. Rev. C **32**, 123 (1985).
5. T. Udagawa and T. Tamura, Phys. Rev. C **29**, 1922 (1984).
6. H. J. Kim *et al.*, Phys. Rev. C **38**, 2081 (1988).
7. J. Wilczynski in *Proceedings of the International Conference on Nuclear Physics*, P. Blasi and R. A. Ricci, eds., Tipografia Compositori, Bologna, Italy, p. 305 (1983).
8. P. H. Stelson *et al.*, Phys. Rev. C **41**, 1584 (1990).

END

DATE FILMED

01 / 10 / 91